Studies of grain orientations and grain boundaries in polycrystalline $SrTiO_3$

Journal of Physics: Conference Series **94** (2008) 012008 doi:10.1088/1742-6596/94/1/012008

Studies of grain orientations and grain boundaries in polycrystalline $SrTiO_3$

Shao-Ju Shih[1], Karleen Dudeck[1], Si-Young Choi[1], Michael Baeurer[2], Michael Hoffmann[2] and David Cockayne[1]

[1]Department of Materials, University of Oxford, Parks Road, Oxford OX1 3PH, United Kingdom

[2]Institut für Keramik im Maschinenbau,Universität Karlsruhe (TH),Haid-und-Neu-Straße 7,D-76131 Karlsruhe, Germany

Abstract

Grain size and grain boundary misorientations of niobium-doped and undoped polycrystalline $SrTiO_3$ have been investigated as a function of sintering time, in order to clarify conflicting reports about grain growth in this material. The observations suggest that the prevalence of both low angle grain boundaries and low energy CSLs are strongly correlated to both abnormal grain growth and sintering time. In addition, GB roughness as a function of sintering time has been investigated.

1. Introduction

In polycrystalline titanate-based ceramics (e.g. $SrTiO_3$ and $BaTiO_3$), grain boundaries (GBs) often play a dominant role in controlling materials properties (e.g. sintering behaviour [1,2], electrical properties [3,4]; several authors have reported that low Σ GBs (e.g. Σ3, Σ 5 and Σ 9) have different positive temperature coefficients compared with general GBs (random large angle misoriented GBs) [5,6]). Upon sintering, in the Ti-excess region ((Sr or Ba)/Ti molar ratio less than 1), the GBs contain continuous liquid films and this liquid assists interface diffusion resulting in fast growth [7]. This process, known as liquid phase sintering, is associated with abnormal grain growth, which occurs by the rapid growth of some grains at the expense of others. By doping with a low concentration of donor atoms (e.g. Nb), the grain growth rate can be increased further [8] by changing the chemical composition (ions and vacancies) near the GB region [9,10].

There are conflicting reports about grain growth in this system. Ernst et al. reported that, in titanate-based ceramics (e.g. $SrTiO_3$, $BaTiO_3$ and $Pb(Zr_xTi_{1-x})O_3$), GBs with Σ3 misorientations are found significantly more frequently than expected for random misorientations [11]. However, Saylor et al. reported a different result to Ernst et al. [11] showing that the GBs with Σ3 misorientations occur

with a random distribution in undoped $SrTiO_3$ [12] , and they commented that the result of Ernst et al. [11] may be due to Fe doping and TiO_2 excess. Seaton and Leach investigated the relationship between the microstructure and the populations of low Σ misorientations (Σ3, Σ5 and Σ 9) for donor-doped (Pb, Sr, and Ca) $BaTiO_3$ during the early stages of sintering (sintered no longer than 1 h) [13,14]. They found that the proportion of low Σ GBs increased during the first 30 min and then became stable. Recent work of Park et al. [15], investigating the Σ misorientations in undoped $SrTiO_3$ as a function of annealing time (1 h and 16 h), came to a different conclusion, finding that the proportion of Σ3 misorientations in undoped $SrTiO_3$ decreased with annealing time.

In order to clarify the situation, this paper investigates (i) grain size distributions and (ii) the geometry of GBs in samples sintered for different times, for both Nb-doped and undoped $SrTiO_3$. Grain misorientations have been determined by electron backscattered diffraction (EBSD), and the roughness of GBs for different sintering times has been studied using high resolution transmission electron microscopy (HRTEM).

2. Experimental Procedure

2.1 Ceramic Synthesis

Nb-doped $SrTiO_3$ powder was prepared from pure powders of 99.9 wt % Nb_2O_5 (ChemPur, Karlsruhe, Germany), 99.9 wt % $SrCO_3$ (Sigma-Aldrich, Milwaukee, United States) and 99.9 wt% TiO_2 (Sigma-Aldrich, Milwaukee, United States, 99.9 wt %). The powder mixture of $99.4SrTiO_3 \cdot 1.2Nb$ (mol%) was ball-milled for 24 h with ethanol using ZrO_2 balls, followed by 20 h drying at 120°C, calcining at 1300 °C in air for 1 h and then ball-milling again. The calcinated powder was sintered at 1420°C in oxygen for 1, 2, 4 and 20 h and then quenched to room temperature. For a blank experiment, undoped $SrTiO_3$ samples were prepared from the same $SrCO_3$ and TiO_2 powders. The powder mixture of 99.6 $SrTiO_3$ (mol %) was followed by the same ball-milling and calcination procedures, and sintered by uniaxially hot pressing at 1420 °C in oxygen for 20 h, and then quenched to room temperature.

2.2 Grain Size and Misorientation

Grain size and grain misorientation analyses were carried out using EBSD. In order to obtain precise misorientation data, it is important to collect good quality Kikuchi maps from EBSD, and this requires a well polished and uncontaminated sample surface. The EBSD samples were prepared by mechanical grinding with SiC abrasive papers (800, 1200, 2000 mesh) and then polishing with a succession of 9, 3, 1 and 0.1 μm diamond cloths. The samples were chemically etched in a $95H_2O$-4HCl-1HF (by volume percent) solution for 30 s to remove surface contamination caused by sample polishing.

EBSD Kikuchi patterns were obtained using a JEM 6300F SEM, with an 80μA beam current, and 0.19-4.64 μm step size, at a working distance of 15 mm. The step size was at least ten times

smaller than the average grain size, to give precise measurements. The sample was inclined at 70° to the 20 kV incident electron beam. Analysis of the Kikuchi patterns was carried out with computer software (Inca, Oxford Instruments, UK). For grain determination, two neighbouring pixels were considered to be in the same grain if they had a misorientation angle less than 3°, and GBs were identified between adjacent grains. The grain size (including large (abnormal) and small grains) and grain size distributions were determined by linear intercept techniques (for details of the technique see [15], [16]). The average grain size G of all grains was calculated by G = grain size of large grains × volume percent of large grains + grain size of small grains × volume percent of small grains. GBs between grains with a misorientation less than 15° were designated as small angle GBs. The number of analyzed grains was larger than 400 for each sample.

3. Results and Discussion

3.1 Microstructure and Grain Orientation

Figures 1 (a)-(d) show the EBSD grain orientation image maps (OIMs) along the sample normal direction with respect to the stereographic triangle (using the colour chart of figure 1 (f)) for 1, 2, 4 and 20 h sintering respectively for the Nb-doped sample, and figure 1 (e) for 20 h sintering for the undoped sample. In this study, all samples had a Ti-excess, which should cause liquid phase sintering and abnormal grain growth [7].

Each of the image maps of figure 1 was converted into a size histogram. As an example, figure 2 shows the histogram corresponding to figure 1(a) (1 h sintering). The average grain size (size here means diameter) is 1.8 μm, with a small outlying number (0.2 % by number and 2.9% by volume) of larger grains of size ~5.1 μm. figure 1b for 2 h sintering has a similar histogram, with both small and large grains. With increasing sintering time, the fraction of large grains increases, as does their average size, but in all cases there is a clear separation between those grains which are small in size, and large grains, and for both the doped and undoped samples. These results are evidence for abnormal grain growth, with grains having a grain size much larger than those in samples with a 1 h sintering time, and in the larger size group in each sample, being identified as those which have undergone abnormal grain growth.

However a comparison between the undoped (figure 1 (d)) and doped (figure 1(e)) samples, sintered under the same conditions and for the same time of 20 h, shows that abnormal grain growth is much faster in the Nb-doped samples than in the undoped samples, with the doped sample having an average grain size of 55.5 μm compared to 2.6 μm for the undoped, and a higher volume percentage of large grains (99.8 vol % compared to 8.6vol %). This result is in agreement with earlier studies which show that different GB growth behaviour can be obtained by modifying the dopants [17].

It is instructive to display the data of figure 1 as grain size as a function of sintering time. Figure

3 shows the average grain size of the two components (large and small) of the size distribution, the average grain size of all grains, and the volume percentage of grains for each component, for different sintering times. For the shortest sintering time (1 h), large grains are not frequently observed (only 0.2 % by number and 2.9% by volume), while for the longest sintering time (20 h), 96.5% by number (99.8% by volume) of grains observed are large. Most of the large grains have a size more than ten times that of the small grains (for 2, 4 and 20 h sintered samples), which implies that the GB mobility of the large grains is at least ten times that of small grains.

3.2 Crystallographic structure

Figure 4 shows the grain misorientation distribution in Nb-doped $SrTiO_3$ samples sintered for 1 h and 20 h. Two significant differences between the two samples can be seen. Firstly, the large fraction of small angle GBs (usually defined as having misorientation angle less than 15°) present in the sample sintered for 1h disappears in the sample sintered for 20h. Secondly, the misorientation distribution for the 20h sintered sample is more like the random (Mackenzie [18,19]) distribution than is the 1h sample, in that not only do the small angle GBs agree more closely with this distribution, but so also do those at ~45°. This can be explained as energy minimization during the liquid phase sintering process as follows. Small angle GBs and CSL GBs are generally of relatively low energy [20,21]. During the first stage of the liquid phase sintering, grains rearrange to a low energy configuration by reorienting high energy GBs into low energy GBs. This accounts for the large number of small angle GBs at the early stages. During liquid phase sintering, further energy minimization can be achieved in two ways (i) by grain growth reducing the GB density. Since large angle GBs are less stable and so more mobile [22], this results in small angle and CSL GBs being consumed by high angle GBs during growth. (ii) by an increase in CSL boundary densities. (Seaton and Leach showed this second effect, where the density of Σ3 grain misorientations (which are low energy and large angle) increased with sintering time between 0 and 60 min in donor doped $BaTiO_3$ [13,14].)

These mechanisms can be applied to the experimental results reported here as follows.

Figure 5 shows the proportion of Σ3 (Brandon criterion [23]) misorientations and small angle GBs of Nb-doped $SrTiO_3$ samples as a function of sintering time. Both small angle and Σ3 misorientation GBs have low energy and reduce in population with increasing sintering time. According to Randle's analysis using the McKenzie distribution [18,19], the Σ3 population for a random distribution of GBs is 1.5 %. Our result for the Σ3 population of the 20 h sintered sample (~1.7 %) is near Randle's figure. The results here appear to be dominated by mechanism (i).

In the case of undoped $SrTiO_3$, the sample sintered for 20 h has a lower proportion (8.6 vol %) of large grains (calculated from figure 1(e)) than the Nb-doped sample (99.8 vol %) (from figure 3). This suggests that the mobility of GBs during abnormal grain growth in undoped samples is less than in Nb-doped samples, and so abnormal grains in the undoped samples have not consumed low energy

GBs (e.g. Σ3 misorientations) from small grains to the same extent as for doped samples. Consequently for undoped $SrTiO_3$ mechanism (i) does not dominate (ii) to the same extent as for doped $SrTiO_3$, and Σ3 misorientations (low energy) are found at a higher proportion (2.8 %) than for doped samples. Thus, in this system, the proportion of low energy GBs (small angle and CSL GBs) is strongly correlated with the grain growth behaviour (e.g. abnormal grain growth).

We now consider the apparently conflicting results in the literature. Ernst et al. reported that Fe doped $SrTiO_3$ had preferred Σ3 misorientations [11] with five Σ3 misorientations being found for 90 measured grain misorientations (6%) based on Brandon's criterion. However, for undoped $SrTiO_3$, Saylor et al. found 1276 Σ3 orientation segments in 75088 grain boundary segments (1.7%), and concluded that in their sample the proportion of Σ3 misorientations was near random [13]. They suggested that the result of Ernst et al. [11] is due to TiO_2 excess and Fe doping. We suggest that this discussion can be resolved by considering abnormal grain growth. From the measurement reported by Ernst et al [11], all 90 measured grains are small grains (<12.5 μm) (the average grain size is 70 μm in Ernst et al.'s sample). These would be low energy GBs from the early sintering stage, and Σ3 preferred misorientations. However, measurements reported by Saylor et al. [13] come from both small (~30-120 μm) and large grains (~240-530 μm). Their results included grains which had undergone abnormal grain growth; therefore, the preferred Σ3 misorienations formed in the early sintering stage may have been consumed and then contributed to a random distribution.

3.3 Grain Boundary Roughness

A study of the GB structures for the different samples was carried out by HRTEM. Specimens were prepared by mechanical grinding to a thickness of ~100 μm, ultrasonically cut into 3 mm disks, dimpled to a thickness of ~15 nm near the specimen centre and then ion-milled in a precision ion polishing system (PIPS, Gatan, Pleasanton, CA) to obtain thin areas for electron transmission. Planar {110} and {100} GBs were frequently observed in both doped and undoped $SrTiO_3$ samples. These boundaries were studied in detail by HRTEM (JEOL JEM-3000F) using an electron energy of 300 keV, and a point resolution of 0.17 nm. An example is shown in figure 6. Careful inspection shows that usually the surface is not atomically flat, but has short {110} and {100} segments. In this sense, the surfaces are rough. To determine the degree of roughness, the average length (unit cells) of {110} and {100} segments were analyzed for three {110} and {100} GBs. The larger the average length of the segment, the flatter the GB surface.

Figures 6(a)-(d) show typical {110} GBs in Nb-doped $SrTiO_3$ for increasing sintering time. A close inspection shows that the {110} GBs from the 1 h sintered sample are nearly atomically flat, composed of {110} segments with a length of 10-20 unit cells and {100} segments with a length of 1-2 unit cells. After several hours sintering, the {100} GBs become rougher, as shown in figure

6(b)-(d). The roughness can be assessed by plotting the relative lengths of {110} and {100} segments as a function of sintering time as in figure 7. The fact that the grains sintered for longer sintering times are rougher, and that rougher grain boundaries (more steps) are more mobile [22] agrees with the observation of increasing large grains with sintering time. In the case of 1 h sintering, most grains are small, and {110} GBs with flat surfaces are frequently observed.

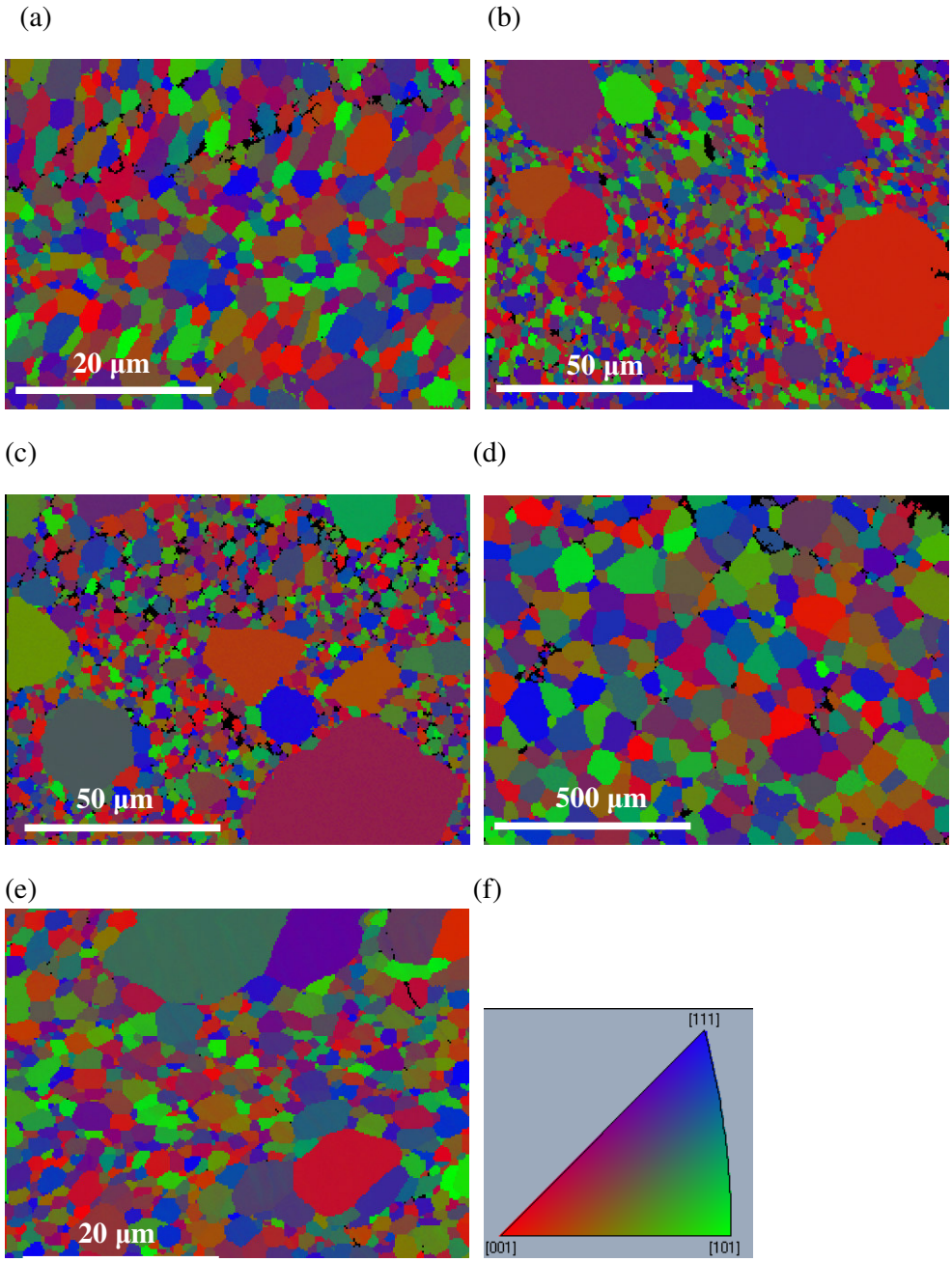

Figure 1. OIMs along the sample normal direction showing the orientation and shape of the grains obtained on Nb-doped $SrTiO_3$ samples sintered for (a) 1 h ,(b) 2 h (c) 4 h and (d) 20 h and the undoped $SrTiO_3$ sample sintered for (e) 20 h. Samples were sintered at 1420 °C in oxygen. Colour-shading in OIMs corresponds to that of the stereographic triangle of (f) and represents the orientation normal to the specimen surface.

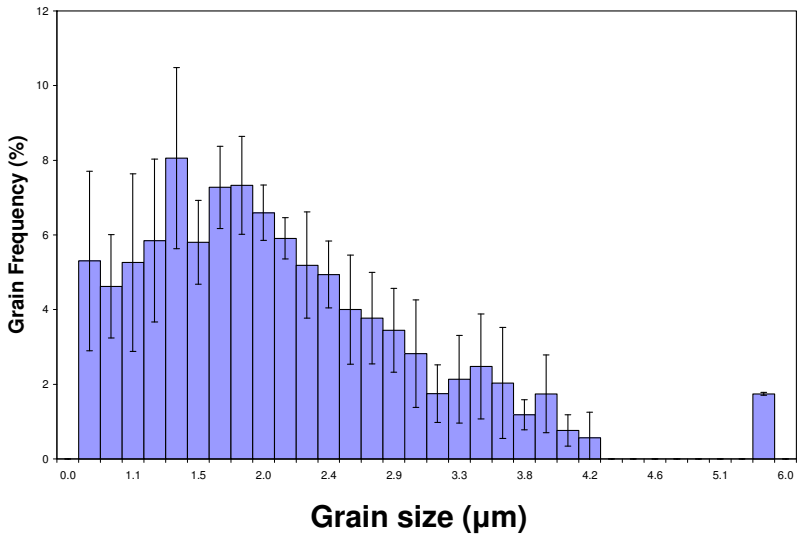

Figure2. The grain size distribution of Nb-doped $SrTiO_3$ samples sintered for 1 h at 1420 °C in oxygen. (Error bars indicate the standard deviation of grain size measurement from three different areas. Each area includes more than 400 grains.)

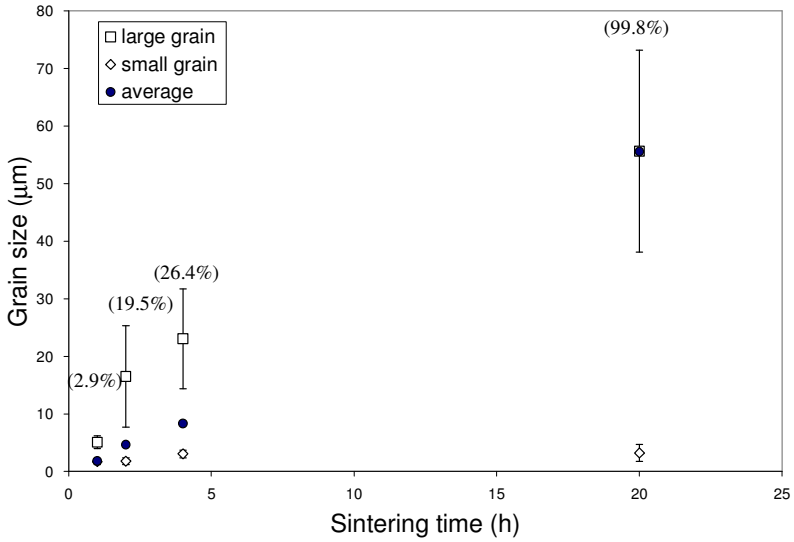

Figure 3. Grain size of Nb-doped $SrTiO_3$ samples as a function of sintering time. Samples sintered at 1420 °C in oxygen. The number in brackets indicates the volume proportion of large grains.

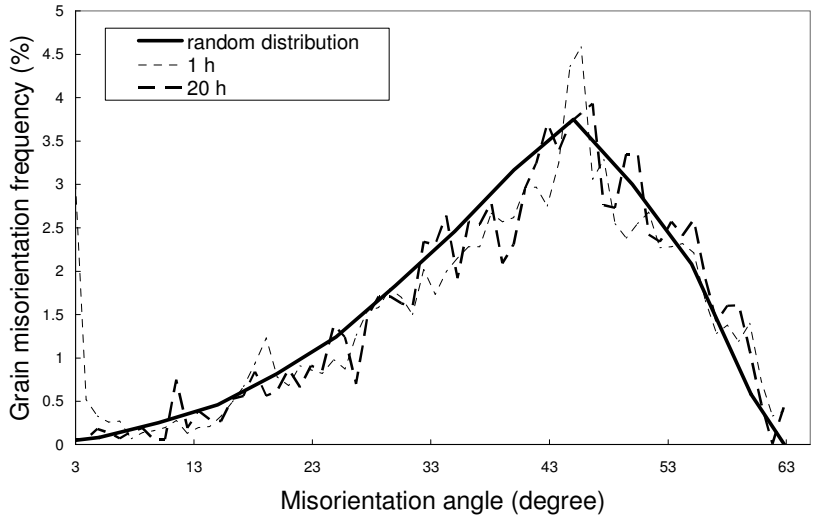

Figure 4. Grain misorientation distribution on Nb-doped $SrTiO_3$ samples sintered for 1 h and 20 h. The samples are sintered at 1420 °C in oxygen. The theoretical random distribution is the Mackenzie distribution (heavy solid line).

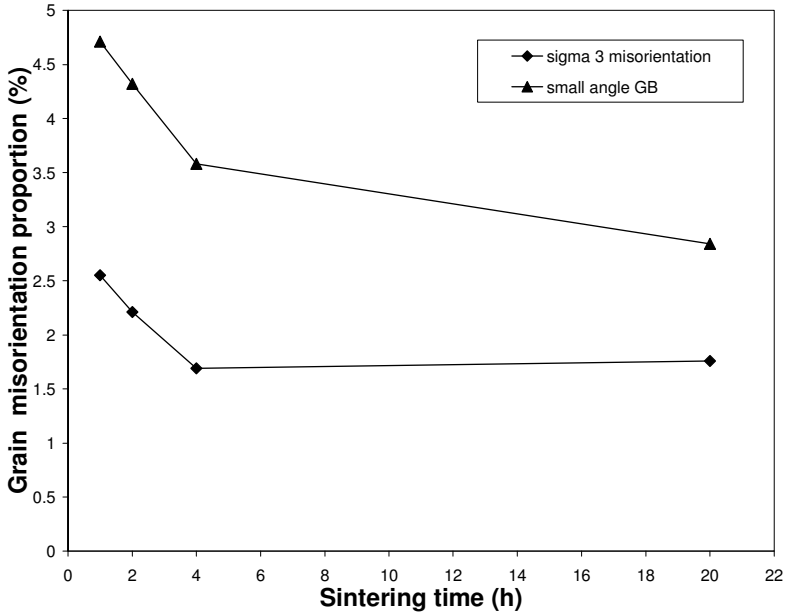

Figure 5. Proportion of sigma 3 misorientations and small angle grain boundaries of Nb-doped $SrTiO_3$ samples as a function of sintering time. Samples were sintered at 1420 °C in oxygen.

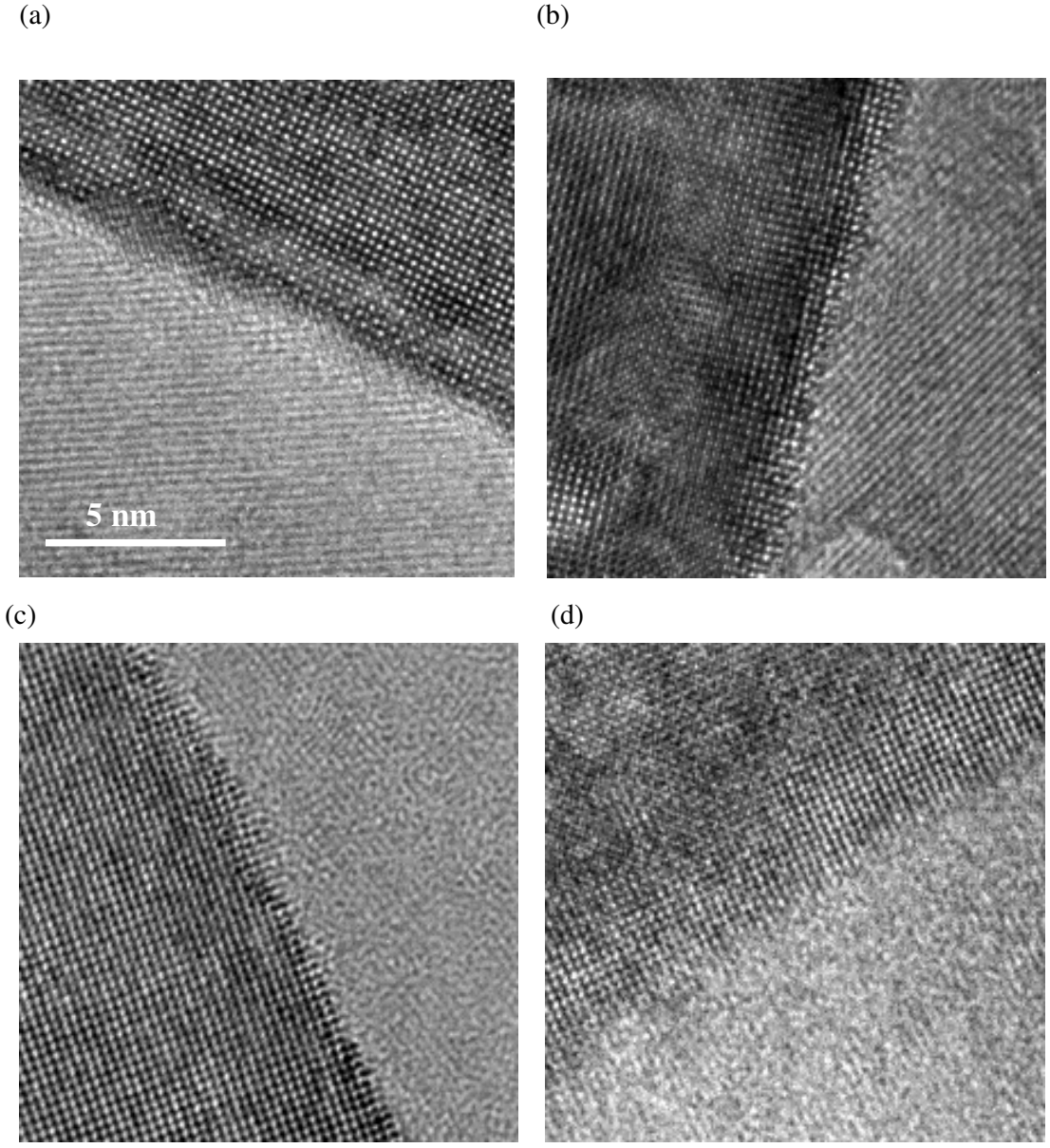

Figure 6. Typical high resolution image of the {110} GB on Nb-doped $SrTiO_3$ samples sintered for (a) 1 h ,(b) 2 h (c) 4 h and (d) 20 h. Samples were sintered at 1420 °C in oxygen.

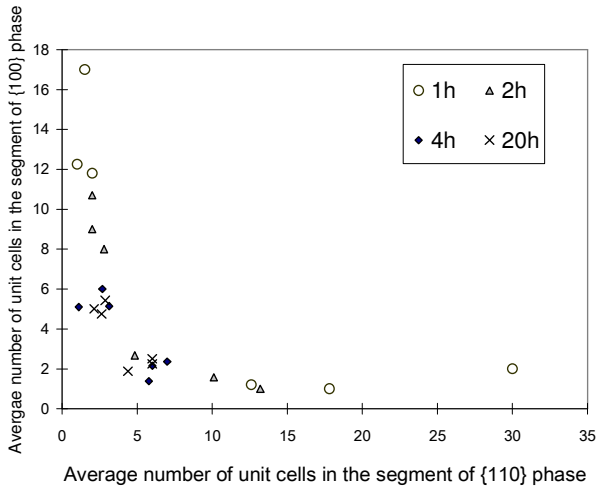

Figure 7. Interface roughness of the {110} and {100} grain boundaries on Nb-doped $SrTiO_3$ samples as a function of sintering time. Samples sintered at 1420°C in oxygen.

4. Conclusion

The frequency of low energy GBs (e.g. low angle GB and Σ3 misorientations) observed in polycrystalline $SrTiO_3$ has been correlated to the sintering conditions. Nb doping increases GB mobility with the proportion of low energy GBs not only determined by sintering conditions but also by the mechanism of abnormal grain growth. GB roughness has been studied as a function of sintering time.

Acknowledgement

The authors thank Dr Nicole Benedek and Profs Mike Finnis and Adrian Sutton for helpful discussions. The authors would like to thank the European Commission for financial support under contract Nr. NMP3-CT-2005-013862 (INCEMS). Mr Shao-Ju Shih wishes to acknowledge the support of the Overseas Student Scholarship (contract No. SAS 952130016) by the Taiwan Government. Ms Karleen Dudeck would like to acknowledge the support of the Oxford University Clarendon Fund and the Canadian Natural Sciences and Engineering Research Council.

References:

[1] Hillert M 1965 *Acta Metall*. **13** 227-38
[2] Hennings D F K, Janssen R and Reynen P J L 1987 *J. Am. Ceram. Soc.* **70** 23-27
[3] Gerthsen P and Hoffmann B 1973 *Sol. State Electr.* **16** 617-22
[4] Yamaji A and Waku S 1972 *Rev. Elect. Comm. Lab.* **20** 747
[5] Ogawa H, Demua M, Yamamoto T and Sakuma T 1995 *Mater. Sci. Lett.* **14** 537-38
[6] Hayashi K, Yamamoto T and Sakuma T 1996 *J. Am. Ceram. Soc.* **79** 1669-72
[7] Chung S Y and Kang S J L 2003 *Acta Mater.* **51**, 2345-54
[8] Bae C, Park J G, Kim Y H and Jeon H 1998 *J. Am. Ceram. Soc.* **11** 3305-09
[9] Chan N H, Sharma R K and Smyth D M 1981 *J. Electrochem. Soc.* **128** 1762-69
[10] Peng C J and Chiang Y M 1987 Variations in grain growth of donor-doped $SrTiO_3$ with cation nonstoichiometry *Materials Science Research* vol 21 (New York: Plenum Press) pp 555-68
[11] Ernst F, Mulvihill M L, Kienzle O and Rühle M 2001 *J. Am. Ceram. Soc.* **84** 1885-90
[12] Saylor D M, Dosler B E, Sano T and Rohrer G S 2004 *J. Am. Ceram. Soc.* **87** 670-76
[13] Seaton J and Leach C 2005 *J. Eur. Ceram. Soc.* **25** 3055-58
[14] Seaton J and Leach C 2005 *Acta Mater.* **53** 2751-58
[15] Park M B, Shih S J and Cockayne D J H 2007 *J. Microsc-Oxford,* **3** 292-97
[16] Wurst J C and Nelson J A 1972 *J. Am. Ceram. Soc.* **55** 109
[17] Chung S Y, Yoon D Y and Kang S J L 2002 *Acta Mater.* **50** 3361-71
[18] Randle V 1999 *Mater. Sci. Technol.* **15** 246-52
[19] Mackenzie J K 1958 *Biometrika* **45** 229–36
[20] Randle V 2004 *Int. Mater. Rev.* **49** 1-11
[21] Dimou G and Aust K T 1974 *Acta Metallurgica* **22** 27-32
[22] Sutton A P and Balluffi R W 1995 *Interface in Crystalline Materials* (Oxford: Oxford University Press)
[23] Brandon D G 1966 *Acta Metall.* **14** 1479-84